Journal of Integrative Agriculture 2026, 25(7): 3086–3089

Available online at ScienceDirect

Journal of Integrative Agriculture



LETTER

TaPRR95 regulates wheat flowering time and yield partially by interacting with the CONSTANS-like protein

Xinxin Cheng[1], Lijun Zhang[2], Ying Xu[1], Yongchao Hao[1, 2], Peng Jiang[4], Shams ur Rehman[2], Shisheng Chen[2], Lingrang Kong[1], Shuxin Zhang[3], Hongwei Wang[1], Yan Zhao[1#], Guiping Wang[2, 3#]

[1] *State Key Laboratory of Wheat Improvement/College of Agronomy, Shandong Agricultural University, Tai'an 271018, China*
[2] *State Key Laboratory of Wheat Improvement/Peking University Institute of Advanced Agricultural Sciences/Shandong Laboratory of Advanced Agriculture Sciences in Weifang, Weifang 261325, China*
[3] *State Key Laboratory of Wheat Improvement/College of Life Sciences, Shandong Agricultural University, Tai'an 271018, China*
[4] *CIMMYT-JAAS Joint Center for Wheat Diseases, Jiangsu Academy of Agricultural Sciences, Nanjing 210014, China*

Highlights

- A *TaPRR95-A* haplotype reduces flowering time and increases grain yield in wheat.
- Protein–protein interaction between TaPRR95-A and TaCOL16-D modulates the *TaFT1*-mediated flowering pathway.
- A validated functional marker enables rapid identification of the target haplotype and provides a practical tool for marker-assisted selection in wheat breeding.

As a staple cereal crop cultivated worldwide, common wheat (*Triticum aestivum* L.) accounts for approximately 35% of global dietary energy requirements (Sharma and Sharma 2025). However, agricultural yields are currently under significant pressure due to the combined impacts of anthropogenic climate change and geopolitical conflicts (Ortiz-Bobea *et al.* 2021; Hultgren *et al.* 2025), which threatens global food security. These challenges necessitate the urgent development of molecular breeding approaches to improve wheat production sustainably.

Previous genetic investigations developed four recombinant inbred line (RIL) populations by crossing the common parental cultivar Yanzhan 1 with three semi-domesticated wheat accessions (Yunnanxiaomai, Yutiandaomai, and Chayazheda 29) and a British cultivar (Hussar). Through multi-environment trials (MET) conducted across five distinct growing seasons and environments (2014–2015: Heze and Tai'an, Shandong Province, China; 2015–2016: Dezhou and Tai'an, Shandong Province, China; 2016–2017: Tai'an), a stable flowering time QTL (*QFD-5A.3*) was identified in combination with meta-QTL analysis (Wang *et al.* 2019; Hu *et al.* 2020). Notably, the circadian rhythm-associated gene *TaPRR95-A* (*CSIAAS5AG0771600HC.mRNA1*), which encodes a pseudo-response regulator protein, is located in a similar genomic region (Chr5A_CS-IAAS_T2T: 542,686,898–542,692,588 bp) (Liu *et al.* 2025). Previous studies have established PRR family genes as key regulators of circadian oscillators (Nakamichi *et al.* 2010; Farré and Liu 2013; Wang *et al.* 2023), photoperiodic responses (Turner *et al.* 2005; Beales *et al.* 2007; Li *et al.* 2020), floral transitions (Liu *et al.* 2024), and inflorescence development (Boden *et al.* 2015).

To explore the functional role of *TaPRR95-A* in regulating flowering time, we generated transgenic wheat lines by introducing *TaPRR95-A* into the Fielder cultivar under control of the maize ubiquitin promoter *via Agrobacterium*-mediated transformation. The *TaPRR95-A* coding sequence was amplified from cDNA of Yanzhan 1, which flowers earliest among the five parental lines. Among the initial five primary transgenic (T_0) plants, three independent overexpression lines (OE-56, OE-59, and OE-61) were selected and advanced to homozygosity in the T_3 generation. These homozygous lines displayed significantly earlier flowering (P<0.01, Student's t-test) under long-day conditions (16 h light/8 h dark), with a reduction in flowering time of 4.38–6.10 days compared to wild-type (WT) plants (Fig. 1-A and B). Quantitative real-time polymerase chain reaction (qRT-PCR) analysis confirmed a substantial upregulation of *TaPRR95* transcripts ranging from 8.98- to 15.34-fold in transgenic plants relative to the WT (Fig. 1-C). Collectively, these findings support the role of *TaPRR95-A* as a positive regulator of the floral transition in wheat.

Received 9 December 2025; Received in revised form 12 February 2026; Accepted 18 February 2026; Available online 24 March 2026
Xinxin Cheng, E-mail: chengxx0120@163.com; #Correspondence Yan Zhao, E-mail: yzhao1216@sdau.edu.cn; Guiping Wang, E-mail: wgp03165@163.com

© 2026 CAAS. Publishing services by Elsevier B.V. on behalf of KeAi Communications Co. Ltd. This is an open access article under the CC BY-NC-ND license (http://creativecommons.org/licenses/by-nc-nd/4.0/). Peer review under responsibility of Editorial Board of *Journal of Integrative Agriculture*.
doi: 10.1016/j.jia.2026.03.051

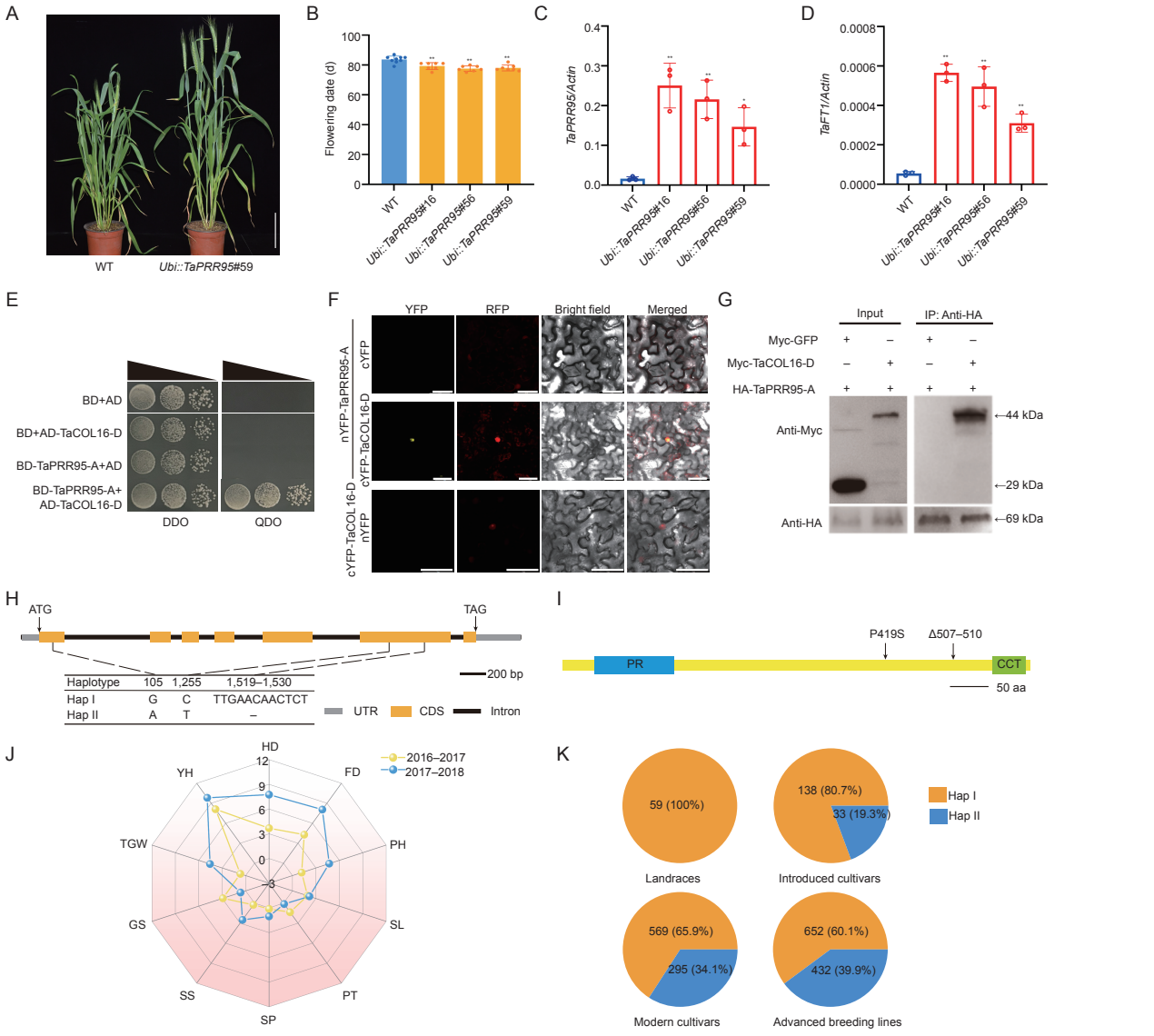


Fig. 1 TaPRR95-A affects wheat flowering time and yield by interacting with TaCOL16-D. A, phenotypic comparison between wild-type (WT) Fielder and *TaPRR95-A* overexpression plants (*Ubi*::*TaPRR95*#59). Scale bar=12 cm. B, flowering date (FD) comparison between WT and *TaPRR95-A* overexpression lines. Data represent mean±SD (n≥7). C and D, transcript levels of *TaPRR95* (C) and *TaFT1* (D) in WT and *TaPRR95-A* overexpression lines. Leaves were sampled from individual plants at the tillering stage. Expression levels were normalized to the housekeeping gene *TaActin* ($2^{-\Delta C_t}$). Data are presented as the mean±SD from three biological replicates. Statistical significance was determined by Student's *t*-test. Asterisks indicate significance levels: *, P<0.05; ** and P<0.01. E–G, protein–protein interactions between TaPRR95-A and TaCOL16-D. Interactions were validated through yeast two-hybrid (Y2H) (E), bimolecular fluorescence complementation (BiFC) (F), and co-immunoprecipitation (Co-IP) assays (G). Black triangles denote protein concentration gradients (1:10 serial dilutions). Media compositions: DDO (SD/–Trp/–Leu) and QDO (SD/–Trp/–Leu/–His/–Ade). Fluorescent tags: yellow fluorescent protein (YFP) and red fluorescent protein (RFP). Scale bar=50 μm. The plus (+) and minus (–) symbols denote the presence or absence, respectively, of co-expressed proteins. H, haplotype analysis of *TaPRR95-A* (*CSIAAS5AG0771600HC.mRNA1*) in the five parental accessions. Orange boxes indicate exons, black lines indicate introns, and gray boxes correspond to untranslated regions (UTRs). The positions of sequence variations between the two haplotypes are indicated by dotted lines. Numerical values indicate the nucleotide positions relative to the coding sequence (CDS), while deletions are indicated by hyphens ('–'). I, predicted protein structure of TaPRR95-A (CSIAAS5AG0771600HC.mRNA1). Sequence variation sites between haplotypes are indicated by arrows. Compared to Haplotype I, Haplotype II results in a proline-to-serine substitution at residue 419 (P419S) and a tetra-amino acid truncation (Δ507–510). J, associations between *TaPRR95-A* haplotypes and yield-related traits. Trait abbreviations: heading date (HD, days), flowering date (FD, days), plant height (PH, cm), spike length (SL, cm), productive tillers per plant (PT), spikelets per panicle (SP), sterile spikelets (SS), grains per spike (GS), thousand-grain weight (TGW, g), and yield per hectare (YH, kg ha^{-1}). Student's *t*-tests were conducted to assess the significance of trait differences between haplotypes. The radar plot shows normalized $\log_{10}$-transformed *P*-values for visual comparison. K, frequencies of the two haplotypes at *TaPRR95-A*. Pie charts show the numbers and percentages of the two haplotypes in landraces, introduced cultivars, modern cultivars, and advanced breeding lines, respectively.

To elucidate the molecular mechanism underlying the acceleration of flowering induced by *TaPRR95-A*, we examined the transcript levels of the florigen gene *TaFT1* in leaves. Comparative qRT-PCR analysis demonstrated a

notable upregulation of *TaFT1* in *TaPRR95-A*-overexpressing transgenic lines compared to the WT (Fig. 1-D), indicating that *TaPRR95-A* facilitates the floral transition by stimulating *TaFT1* expression. Nevertheless, yeast one-hybrid assays did not reveal direct binding between TaPRR95-A and the *TaFT1* promoter (Appendix A), suggesting that the regulatory process is probably indirect and may involve intermediary elements. To identify potentially interacting partners, a yeast two-hybrid (Y2H) screen was conducted using TaPRR95-A as bait, which led to the identification of two CONSTANS-like interactors: CSIAAS7DG0564800HC (TaCOL13-D) and CSIAAS4DG0432200HC (TaCOL16-D; Fig. 1-E, Appendices B and C). The interactions were subsequently validated through bimolecular fluorescence complementation (BiFC) assays in epidermal cells of *Nicotiana benthamiana*, which confirmed the nucleus-localized interactions between TaPRR95-A and both TaCOLs (Fig. 1-F; Appendix D). Furthermore, co-immunoprecipitation (Co-IP) assays confirmed the *in vivo* interaction between HA-tagged TaPRR95-A and Myc-tagged TaCOL16-D (Fig. 1-G). Collectively, these orthogonal interaction assays established the interaction between TaPRR95-A and TaCOL16-D.

The precise regulation of flowering time is crucial for the ecological adaptation and yield maximization of wheat in various agroecosystems. Previous studies have identified key regulators such as the *Ppd1* (Boden *et al.* 2015) and *COL* genes (Zhang *et al.* 2022) in controlling grain yield through meristem determinacy. In *Arabidopsis*, PRR proteins (e.g., PRR9) function as critical nodes within the circadian regulatory network (Matsushika *et al.* 2007; Niinuma *et al.* 2008). In wheat, *TaPRR95-B* was identified as a significant regulator of plant height and heading date through genome-wide association analysis and CRISPR/Cas9-generated mutants (Fu *et al.* 2024). Our investigation pinpointed *TaPRR95-A* as another evolutionarily conserved flowering regulator in wheat. It operates by activating the florigen pathway and directly interacting with CONSTANS-like proteins. Notably, functional divergence or regulatory complexity may occur among different copies of *TaPRR95*, since both the triple mutant of loss-of-function *prr95*^{aabbdd} (Fu *et al.* 2024) and its overexpression lines of *TaPRR95-A* resulted in flowering up to 6 days earlier than the WT plants. Furthermore, differences in the mechanisms between *Arabidopsis* and wheat are evident. In *Arabidopsis*, PRR proteins stabilize CO through direct interactions that enhance its DNA-binding affinity with *FT* promoters (Hayama *et al.* 2017); whereas in wheat, TaCOL16-D directly binds the *TaFT1* promoter (Appendix E). However, the mechanism through which TaCOL16–TaPRR95 interactions influence *TaFT1* promoter affinity remains unclear.

The *TaPRR95-A* gene consists of seven exons and six introns (Fig. 1-H), and it encodes a 607-amino-acid protein with an N-terminal pseudo-receiver (PR) domain (residues 41–144), and C-terminal CO, CO-like, and TOC1 (CCT) domains (residues 558–601; Fig. 1-I). The *TaPRR95-A* gene was amplified from five parental accessions and Chinese Spring (the reference cultivar), and then subjected to comparative sequence analysis using MEGA v7. Sequence alignment identified two distinct haplotypes among these accessions. Yanzhan 1 and Chayazheda 29 are known for their shortest heading and flowering dates among the parental cultivars (Hu *et al.* 2020) and were found to form Haplotype II (Appendix F). Compared to Haplotype I, Haplotype II harbors two non-synonymous single nucleotide polymorphisms (nsSNPs: G105A and C1255T) leading to a proline-to-serine substitution at residue 419 (P419S) and a 12 bp deletion at positions 1,519–1,530, resulting in a four-amino-acid truncation (Δ507–510) (Fig. 1-H and I; Appendices F and G). Subsequently, Y2H assays revealed that both of the TaPRR95-A haplotypes, Haplotype I and Haplotype II, interact with both TaCOL13-D and TaCOL16-D (Appendix H). However, no significant differences were detected in their interaction strengths or patterns. Thus, the functional divergence between the two haplotypes is not likely to be driven primarily by differential binding to TaCOL13-D or TaCOL16-D. Instead, it may involve alternative mechanisms such as interactions with other proteins, differences in protein stability, subcellular localization, transcriptional regulation, or post-translational modifications.

To evaluate the agronomic potential of *TaPRR95-A*, a codominant insertion/deletion (InDel) marker (*95F1R1*) was specifically designed to detect the 12 bp deletion (Appendices F, I and J). A global wheat diversity panel of approximately 2,000 lines was assessed over two consecutive growing seasons (1,822 lines during 2016–2017 and 2,122 lines during 2017–2018) under field conditions. Ten yield-related traits, encompassing two phenological stages (heading and flowering) and three yield components (grains per spike, thousand-grain weight, and grain yield per hectare), were measured. Genotyping using the codominant InDel marker *95F1R1* revealed significant associations between the haplotypes and phenotypes (Fig. 1-J). Lines carrying Haplotype II demonstrated enhanced agronomic performance, and displayed the most robust correlations with grain yield ($-\log_{10}P$=8.10 in 2016–2017 and 9.82 in 2017–2018; Fig. 1-J). Compared to Haplotype I, lines with Haplotype II exhibited earlier flowering by 0.52–0.73 days (P=5.26×10^{-5} and 9.01×10^{-9} for the respective seasons), providing more ample grain filling time and a yield advantage of 450.38–597.54 kg ha^{-1} (P=1.52×10^{-10} and 8.00×10^{-9} for the respective seasons) (Table 1; Appendix K). This yield increase indicates that under current production conditions, the widespread adoption of Haplotype II could boost wheat yields by about 8 to 12%. We then analyzed the frequencies of the two haplotypes across all collected common wheat lines, including 54 landraces, 138 introduced cultivars, 751 modern cultivars, and 1,092 advanced breeding lines. The results revealed a greater frequency of Haplotype II throughout these four types of lines, suggesting positive selection during modern breeding (Fig. 1-K).

Most importantly, this study developed an InDel marker that can be directly applied to molecular design breeding in wheat. It enables precise haplotype selection and rapid identification of superior early-maturing and high-yielding traits, thereby providing “genetic power” for the green and high-quality development of agriculture. Our findings confirm that *TaPRR95-A* is the causal gene underlying wheat flowering time and yield, and we offer a practical molecular marker for the precise breeding of high-yielding wheat varieties.

Table 1 Statistical analysis of the phenotypic data for 10 yield-related traits associated with the *TaPRR95-A* haplotypes in bread wheat under two sowing conditions[1)]

Category[2)]	HD (d)	FD (d)	PH (cm)	SL (cm)	PT	SP	SS	GS	TGW (g)	YH (kg ha^{-1})
2016–2017-Average (II)	187.29	191.75	83.44	9.46	16.01	20.81	1.24	56.44	40.73	6,814.89
2016–2017-Average (I)	187.68	192.27	85.09	9.64	15.55	20.79	1.22	57.83	40.45	6,217.35
2016–2017-Pheno	0.39	0.52	1.65	0.18	–0.46	–0.02	–0.02	1.39	–0.28	–597.54
2017–2018-Average (II)	187.32	191.78	72.39	8.55	14.17	18.13	0.62	50.21	47.62	6,347.50
2017–2018-Average (I)	187.95	192.51	75.20	8.73	14.23	18.31	0.70	50.70	46.28	5,897.12
2017–2018-Pheno	0.63	0.73	2.81	0.18	0.06	0.18	0.08	0.49	–1.34	–450.38

[1)] HD, heading date; FD, flowering date; PH, plant height; SL, spike length; PT, productive tillers per plant; SP, spikelets per panicle; SS, sterile spikelets; GS, grains per spike; TGW, thousand-grain weight; YH, yield per hectare.
[2)] The II genotype represents *TaPRR95-A*^{HapII} and the I genotype represents *TaPRR95-A*^{HapI}. Pheno, differences in the 10 yield-related traits between the two *TaPRR95-A* haplotypes.

Acknowledgements

The authors thank the transformation facility at the Shandong Agricultural University for their assistance with the wheat genetic transformation. This study was supported by the Key R&D Program of Shandong Province, China (2023LZGC022), the Shandong Provincial Natural Science Foundation, China (ZR2023QC103), and the National Natural Science Foundation of China (U23A20181).

Declaration of competing interest

The authors declare that they have no conflict of interest.

Declaration of generative AI and AI-assisted technologies in the writing process

During the preparation of this manuscript, the authors used DeepSeek-V3.2 to assist in improving the clarity and readability of the language. All content generated was carefully reviewed and revised by the authors as necessary, and the authors take full responsibility for the final content of this article.

Appendices associated with this paper are available at https://doi.org/10.1016/j.jia.2026.03.051

References

Beales J, Turner A, Griffiths S, Snape J W, Laurie D A. 2007. A *Pseudo-Response Regulator* is misexpressed in the photoperiod insensitive *Ppd-D1a* mutant of wheat (*Triticum aestivum* L.). *Theoretical and Applied Genetics*, **115**, 721–733.

Boden S A, Cavanagh C, Cullis B R, Ramm K, Greenwood J, Jean Finnegan E, Trevaskis B, Swain S M. 2015. *Ppd-1* is a key regulator of inflorescence architecture and paired spikelet development in wheat. *Nature Plants*, **1**, 1–6.

Farré E M, Liu T. 2013. The PRR family of transcriptional regulators reflects the complexity and evolution of plant circadian clocks. *Current Opinion in Plant Biology*, **16**, 621–629.

Fu M, Liu S, Che Y, Cui D, Deng Z, Li Y, Zou X, Kong X, Chen G, Zhang M, Liu Y, Wang X, Liu W, Liu D, Geng S, Li A, Mao L. 2024. Genome-editing of a circadian clock gene *TaPRR95* facilitates wheat peduncle growth and heading date. *Journal of Genetics and Genomics*, **51**, 1101–1110.

Hayama R, Sarid-Krebs L, Richter R, Fernández V, Jang S, Coupland G. 2017. PSEUDO RESPONSE REGULATORs stabilize CONSTANS protein to promote flowering in response to day length. *The EMBO Journal*, **36**, 904–918.

Hu J, Wang X, Zhang G, Jiang P, Chen W, Hao Y, Ma X, Xu S, Jia J, Kong L, Wang H. 2020. QTL mapping for yield-related traits in wheat based on four RIL populations. *Theoretical and Applied Genetics*, **133**, 917–933.

Hultgren A, Carleton T, Delgado M, Gergel D R, Greenstone M, Houser T, Hsiang S, Jina A, Kopp R E, Malevich S B, Mccusker K E, Mayer T, Nath I, Rising J, Rode A, Yuan J. 2025. Impacts of climate change on global agriculture accounting for adaptation. *Nature*, **642**, 644–652.

Li N, Zhang Y, He Y, Wang Y, Wang L. 2020. Pseudo response regulators regulate photoperiodic hypocotyl growth by repressing PIF4/5 transcription. *Plant Physiology*, **183**, 686–699.

Liu S, Li K, Dai X, Qin G, Lu D, Gao Z, Li X, Song B, Bian J, Ren D, Liu Y, Chen X, Xu Y, Liu W, Yang C, Liu X, Chen S, Li J, Li B, He H, *et al.* 2025. A telomere-to-telomere genome assembly coupled with multi-omic data provides insights into the evolution of hexaploid bread wheat. *Nature Genetics*, **57**, 1008–1020.

Liu Z, Liu W, Wang Z, Xie Z, Qi K, Yue D, Li Y, Zhang S, Wu J, Wang P. 2024. Molecular characterization of *PSEUDO RESPONSE REGULATOR* family in Rosaceae and function of *PbPRR59a* and *PbPRR59b* in flowering regulation. *BMC Genomics*, **25**, 794.

Matsushika A, Murakami M, Ito S, Nakamichi N, Yamashino T, Mizuno T. 2007. Characterization of circadian-associated pseudo-response regulators: I. Comparative studies on a series of transgenic lines misexpressing five distinctive PRR genes in *Arabidopsis thaliana*. *Bioscience*, *Biotechnology*, *and Biochemistry*, **71**, 527–534.

Nakamichi N, Kiba T, Henriques R, Mizuno T, Chua N H, Sakakibara H. 2010. PSEUDO-RESPONSE REGULATORS 9, 7, and 5 are transcriptional repressors in the *Arabidopsis* circadian clock. *The Plant Cell*, **22**, 594–605.

Niinuma K, Nakamichi N, Miyata K, Mizuno T, Kamada H, Mizoguchi T. 2008. Roles of *Arabidopsis PSEUDO-RESPONSE REGULATOR* (*PRR*) genes in the opposite controls of flowering time and organ elongation under long-day and continuous light conditions. *Plant Biotechnology*, **25**, 165–172.

Ortiz-Bobea A, Ault T R, Carrillo C M, Chambers R G, Lobell D B. 2021. Anthropogenic climate change has slowed global agricultural productivity growth. *Nature Climate Change*, **11**, 306–312.

Sharma K, Sharma P K. 2025. Wheat as a nutritional powerhouse: Shaping global food security. In: Meena V S, Jaiswal J P, Jinger D, Paramesh V, eds., *Triticum-The Pillar of Global Food Security*. *Agricultural Sciences*. IntechOpen Publishing, London, UK.

Turner A, Beales J, Faure S, Dunford R P, Laurie D A. 2005. The pseudo-response regulator *Ppd-H1* provides adaptation to photoperiod in barley. *Science*, **310**, 1031–1034.

Wang X, Dong L, Hu J, Pang Y, Hu L, Xiao G, Ma X, Kong X, Jia J, Wang H, Kong L. 2019. Dissecting genetic loci affecting grain morphological traits to improve grain weight *via* nested association mapping. *Theoretical and Applied Genetics*, **132**, 3115–3128.

Wang X, Zhang J, Liu X, Kong Y, Han L. 2023. The roles of the *PSEUDO-RESPONSE REGULATORs* in circadian clock and flowering time in *Medicago truncatula*. *International Journal of Molecular Sciences*, **24**, 16834.

Zhang X, Jia H, Li T, Wu J, Nagarajan R, Lei L, Powers C, Kan C C, Hua W, Liu Z, Chen C, Carver B F, Yan L. 2022. *TaCol-B5* modifies spike architecture and enhances grain yield in wheat. *Science*, **376**, 180–183.

Executive Editor-in-Chief Xueyong Zhang
Managing Editor Ning Wang